OpenAccessPub

Research Article | International Journal of Coronaviruses ISSN: 2692-1537 | Freely Available Online

Marginal SARS-CoV-2 Spike Protein Increases Interferon and Balances Cytokine Gene Expression

Satadal Das[1,*], Debasmita Chatterjee[1], Krishnendu Paira[1]

[1]Genetic Research Unit, Heritage Institute of Technology, Kolkata-700107

Corresponding author:

Satadal Das, Genetic Research Unit, Heritage Institute of Technology, Kolkata-700107, ORCID: 0000-0002-9843-3466

Keywords: SARS-CoV-2, RBD antigen, cytokine balance, INF-α, INF-β.

Received: Aug 29, 2022

Accepted: Sep 08, 2022

Published: Oct 01, 2022

Editor:

Raul Isea, Fundación Instituto de Estudios Avanzados -IDEA

Running Title:

SARS-CoV-2 spike protein balances cytokine gene expression

DOI:

10.14302/issn.2692-1537.ijcv-22-4296

Abstract

Some evidence confirms the paradoxical beneficial role of harmful antigens when used in highly diluted forms. In this experiment, we observed cytokine gene expression changes in *Gallus gallus* embryo after challenge with Delta SARS-CoV-2 RBD spike protein antigen, from a concentration of 10 µg/mL to a series of highly diluted forms in ethanol, along with controls. We have also studied pre-and post- experimental combined sets of higher (10 µg/mL) and significantly lower antigen concentrations (attogram level). Attogram and zeptogram level concentrations of the antigen showed consistently remarkable up-regulation of INF-α among different cytokine gene expressions. INF-β gene expressions at the zeptogram level of the antigen showed consistent changes, although not so outstanding. The pre-experimental set having attogram level antigen administered first, followed by a 10µg/mL antigen challenge, showed excellent cytokine balance. Other experimental groups, including the control sets, showed variable results at different concentrations.

Introduction

The records of the past pandemics confirm maximum fatality (~200 million) due to Black Death or bubonic plague from 1347 to1351. Although the ongoing (Fourth wave) or probably ending Covid-19 pandemic has already claimed more than 6 million lives, it is alarming considering the present advancement of medical science. This pandemic divides the world into unequal outcome landscapes [1, 2]. *The Lancet* observed that what emerges next in Covid-19 will depend on the mutations, safety measures of citizens, the policy of the Govern-

ments, progress in the development of vaccines and treatment plans, and not the least, the coordinated activities of different disciplines of the science and humanities[3].

Two critical complications of Covid-19 are acute respiratory distress syndrome (ARDS) and cytokine storm syndrome (CSS)[4]. CSS is marked by a progressive increase of pro-inflammatory cytokines associated with a futile rise of counteracting anti-inflammatory cytokines. If this rise of anti-inflammatory cytokines is too high, it may lead to immune paralysis. An increase in a considerable array of pro-inflammatory cytokines (IL-6, IL-2, IL-8, IL-17, IL-1β, G -CSF, GM-CSF, MCP-1, MIP-1α, TNF-α, IP-10, etc.) is commonly found in COVID-19 [5-7].

The natural binding of coronaviruses' spike (S) glycoprotein occurs with various receptors - ACE2, APN, DPP4, CEACAM, Sia, and O-acSia of human cells. This host-specific binding of the spike protein initiates coronavirus infection. The SARS-CoV-2 spike protein is a significant type 1 trans-membrane protein with two subunits, S1 and S2. The S1 subunit contains a receptor binding domain or RBD that binds with the specific receptors, while the S2 subunit helps membrane fusion. The S protein generates neutralizing - antibodies, protective immunity, and T-cell responses. From the alignment studies, we learned that the RBD sequences lie between the residues 331 and 524 of the S protein [8]. The S2 subunit has three operational domains- fusion peptide, heptad repeat 1, and heptad repeat 2. The dynamic configuration of the immune-active S protein happens when the S1 protein trimer aligns on top of the trimeric S2 [9]. However, spike protein conformational masking and glycan shielding are critical ways that coronaviruses evade host immune response. The crucial step of receptor binding depends on the closed and open conformations of the S-Protein ectodomain trimer [10,11].

The molecular mass of the purified RBD protein is about 34 kDa, which appears densely glycosylated, as the calculated molecular mass of the RBD amino acid sequence alone is ~ 27 kDa. Excess N-glycosylation sites on asparagine over O-glycosylation sites are commonly demonstrated. RBD - ACE2 binding occurs with high affinity. Lymphocytes isolated from vaccinated mice can induce increased levels of cytokines by recombinant RBD *in vitro*. The RBD, thus a good immunogen, triggers a neutralizing antibody response much better than the whole S1 subunit [12]. S2 subunit cannot induce neutralizing antibodies.

Again some virus infections occur quickly when cytokines are elevated. This is facilitated by rising cytokines by active proteases, enhanced cell motility through actin-cytoskeletal pathways, and epidermal cell differentiation along cornified envelope pathways [13]. A critical example is the increased levels of inflammatory cytokines in the female reproductive tract. We find altered expression of proteases, mucosal barrier proteins, and an influx of target cells [14]. This is because proteases are associated with many cytokines like IL-8, IL-1β, GM-CSF, MIP 3α, and IL-17.

As chick embryo has ACE2 receptor (Chicken ACE2), and there are chances of recombinant RBD protein of SARS-CoV-2 to bind with it producing immunological changes, we designed our study to observe cytokine changes within 72 h in this model, with different concentrations of the RBD protein.

Materials and Methods

The Antigen

Recombinant Delta SARS-CoV-2 spike RBD (L452R, E484Q, ABclonal, Lot: 9621050601, Cat. No. RPO2266, Code: WH192258) protein was used in this study. This recombinant protein was produced in HEK 293 expression system. The target protein was made up of the RBD sequence (Arg 319-Phe 541), which was bound to a poly-histidine tag at the C-terminus with mutations L452R, E484Q (Accession #YP-009724390.1). The mutations were identified as variant B.1.617.The lyophilized protein was 0.22µm filtered solution in PBS, pH 7.4, and it produced a band in SDS-PAGE at 35 kDa.

The Embryonated Eggs and The Experiment

Pathogen-free 13- day old embryonated *Gallus gallus domesticus* chicken eggs were procured from

Government State Poultry Farm, Kolkata, India. The surface of the eggs was cleaned with distilled water; all the eggs were candled and incubated at 38°C in 60-80 per cent humidity. In this experiment, we serially diluted the antigen (10 µg/mL in PBS) 1:100 in alcohol in each step, with stroke or agitation, till it was at yoctogram (yg) level. The stroke is important because it led to uniform mixing and showed promising results in our pilot study. On the 14th day, the eggs were arranged in seven experimental sets with five eggs in each group - original antigen (10 µg/mL in PBS), ultra diluted antigen (initial experiments were done by serial dilution of the antigen up to yoctogram level, and the final pre- and post- experimental set studies were done with attogram level antigen, which was found most effective), along with standard control, vehicle alcohol control, stroked vehicle alcohol control, and stroked antigen in alcohol control. In the pre-experimental set, attogram level stroked antigen was injected first, followed by the original antigen after one hour incubation. In the post-experimental group, the original antigen was injected first, followed by stroked antigen at attogram level after one hour incubation. The antigen was also similarly diluted in water and studied for comparison with alcohol as diluents. However, it was observed that the protein molecules degraded rapidly in water. Except for the standard control in all groups, 100 µL of each material was injected through the amniotic route, and all sets were studied in triplicates. Inoculated eggs were candled the next day, rotated three times a day, and incubated as before. All eggs were harvested after 48 h (on 16th day) after exposure to 2-8°C for two hour. 5-10 mL of allantoic fluids and 0.5-1 mL of amniotic fluids were collected in sterile vials and stored at - 80° C for further analysis. All embryos were then dissected to collect liver for histopathological study by hematoxylin and eosin (H&E) stain.

Molecular Biology Analysis

The total RNA was extracted from the allantoic fluid using RNA isoplus from all the samples. The RNA was quantified using a UV-Vis spectrophotometer by A260/A280 ratio. cDNA was synthesized with the purified RNA using a cDNA synthesis kit with conventional PCR. The primer annealing temperature was standardized at 55 - 58ºC using gradient PCR. A gel run of the PCR products was carried out to confirm the annealing temperature. Comparative gene expression studies were done in real-time PCR (Bio-Rad CFX96, Singapore) with SYBR Green tagged primers, dNTPs, Taq polymerase, MgCl2, buffer, etc. The changes of expressions were calculated as fold increase or decrease from the value of the standard control and compared with the housekeeping gene β-actin. We studied cytokine gene expressions of INF-α, INF-β, INF-γ, IL-6, IL-8, IL-10, IL-1β, TGF-β1.

Physical Properties Study of Ultra Diluted (Attogram Level) Stroked Antigen in Alcohol

In this study, we used dynamic light scattering photon correlation spectroscopy (Zeta potential) with Malvern Zeta Sizer (Nano series) ZEN 3600 (United Kingdom). It primarily measures macromolecular Brownian motion due to solvent molecular bombardment on them. It indicates the difference in potential between the fluid layer with oppositely charged ions associated with the particle surface and the dispersant (ethanol). It is used mainly for formulations of protein solutions, suspensions, etc. HPLC study was done with Agilent Technologies Instrument. SEM study was done with CRNN Zeiss SEM instrument. UV-Spectra study was done with Agilent Carrywin 60 UV-Vis Spectrophotometer (Malaysia) to find any difference between UV-spectra of the attogram level antigen and the vehicle alcohol.

Results

Allantoic Fluid Study Results

It is important to note that all cytokine gene expression changes in this experimental model occurred at 48h of incubation. There were no cytokine gene expression changes at 24h and 72h, which we observed in our pilot study.

With attogram and zeptogram levels of spike protein RBD, IFN-α gene expression was remarkably increased (Figure 1). This exciting finding was uniform in all repeat examinations. IFN-β gene expression was also mildly but constantly (Figure 3) boosted with attogram level antigen. At

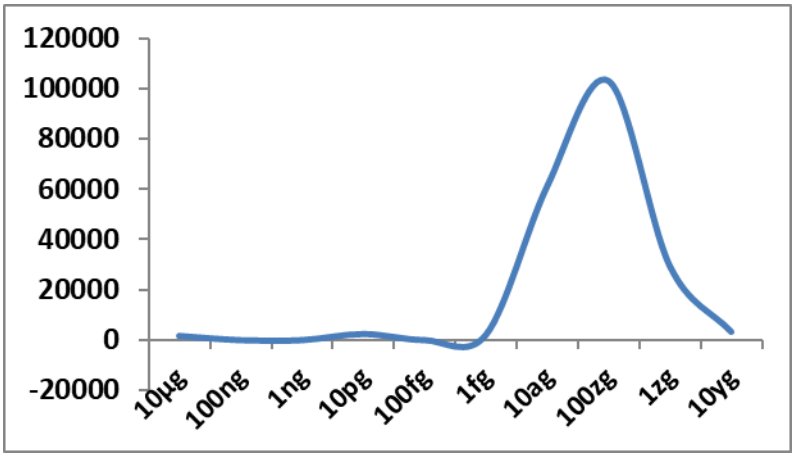

Figure 1. IFN-α gene expression changes (Y axis) in allantoic fluid of embryonated eggs at 48h after challenge with different concentrations of Delta spike protein RBD antigen of SARS-CoV-2; fg-femtogram, ag-attogram, zg-zeptogram, yg-yoctogram.

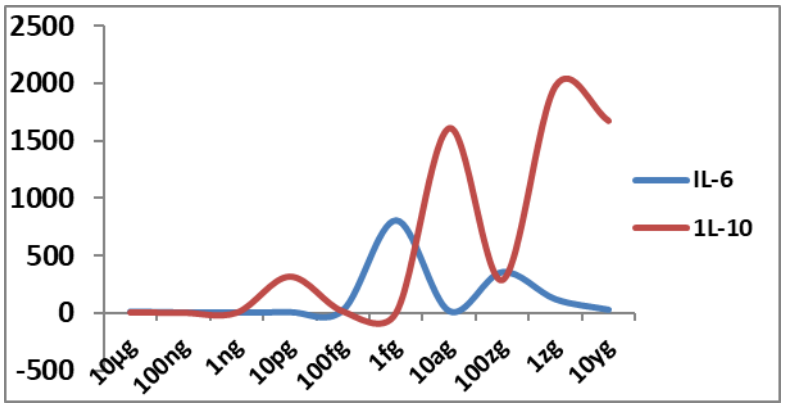

Figure 2. IL-6 and IL-10 gene expression changes (Y-axis) at 48h with different concentrations of Delta spike protein RBD antigen of SARS-CoV-2 in allantoic fluid of embryonated egg; fg-femtogram, ag-attogram, zg-zeptogram, yg-yoctogram.

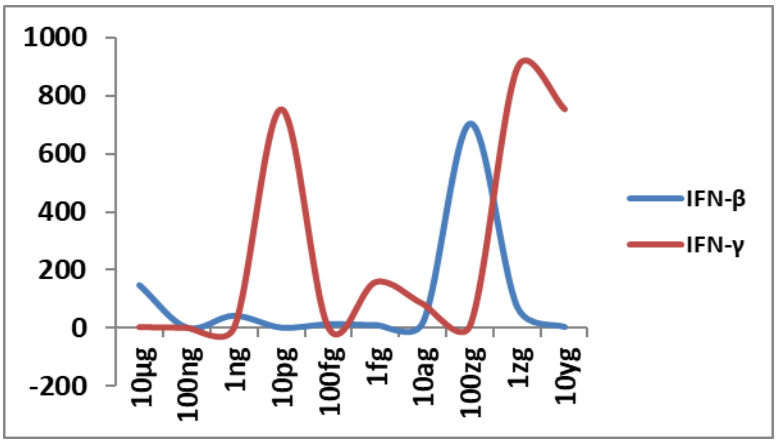

Figure 3. IFN-β and IFN-γ gene expression changes (Y-axis) at 48h with different concentrations of Delta spike protein RBD antigen of SARS-CoV-2 in allantoic fluid of embryonated egg; fg-femtogram, ag-attogram, zg-zeptogram, yg-yoctogram.

the attogram level, IL-10 gene expression was more than IL-6 (Figure 2), indicating the possibility of this anti-inflammatory cytokine's reasonable control of pro-inflammatory cytokines. INF-γ gene expression was more at picogram and zeptogram levels. Other cytokine changes were very mild (Figure 4).

In the pre-experimental set where antigen in attogram level was administered first, followed by 10 µg/mL antigen challenge after 1h, there were significantly increased gene expressions of IFN-α (5423 fold) and IFN-γ (1089 fold); mild to moderate increase of IFN-β (429 fold), IL-10 (77 fold) and IL-6 (30 fold). The cytokine balance appeared good as anti-inflammatory cytokine gene expression was more than pro-inflammatory cytokine gene expressions.

In post-experimental set where 10 µg/mL antigen challenge was done first, followed by attogram level antigen after 1h, significantly increased gene expression of IFN-α (6630 fold), a moderate increase of IFN-β (240 fold) and IFN-γ (126 fold) with a mild increase of IL-6 (33 fold) and IL-8 (14 fold) gene expressions were found. However, IL-10 gene expression was not increased, indicating a possible cytokine imbalance with increased pro-inflammatory cytokines.

With alcohol, mildly increased IFN-α (116 fold), IFN-β (36 fold), and IL-6 (59 fold) gene expressions were found. When water was used as a vehicle, we observed better results when studied immediately after dilution. In this experiment, we observed a marked increase of IFN-γ (14647 fold), 1L-10 (4438 fold), and IFN-α (2881 fold); mild to moderately increased gene expressions of IL-6 (100 fold) and IFN-β (59 fold) with stroked attogram level dilution of antigen in water. However, there were many variations, and thus we used alcohol for dilutions in our main experiments.

Another critical point to note was that in experiments with stroked and non-stroked attogram level antigens, the main difference was IFN-α and IFN-γ gene expressions (Figure 5); IFN-α gene expression was markedly increased with stroked antigen, while IFN-γ gene expression was significantly increased with non-stroked antigen.

Amniotic Fluid Results

We studied amniotic fluid changes as we injected through the amniotic route. However, most cytokine changes were mild (except IL-6, Table1) and not uniform. All three interferons tested in this experiment were increased mildly with attogram level stroked antigen. IL-1β was also mildly increased in pre-, post-experimental sets and antigen sets.

Histopathological Study of The Liver

In the control set, authentic lobular architecture was absent, as usual in chick embryos. Mass of hepatocyte plates was present along with sinusoids. Some encapsulated nodular aggregates of lymphocytes were also not unusual in normal chick embryos. With 10µg/mL, antigen features of acute hepatocellular degeneration and necrosis with infiltration of heterophile, immature granulocytes and lymphocytes were present. There was also intravascular fibrin thrombus at a few places. In post-experimental and alcohol control sets, we also observed similar findings to a moderate degree. Histopathological features were identical to standard control in attogram-level antigens and pre-experimental groups.

In the physical properties study with attogram level stroked antigen in alcohol, we observed Zeta potential at -1.19 mV, the dispersant ethanol was with dielectric constant 24.3, and Zeta deviation was 9.60 mV. This indicated the dispersed particles were predominantly negatively charged and unstable, and likely to aggregate. Thus we used freshly prepared dilute antigens in each experimental set. HPLC study chromatogram (Figure 6) showed 11 peaks with trace amounts of chemicals, which extends from 1.626 to 4.414 Ret. Time (280 nm) and the area extended from1233 to 4471. This indicated the presence of chemicals at attogram level dilutions, although we could not specify the substances at this stage. SEM study revealed the presence of antigen nanoparticles (Figure 7). UV-spectroscopy could not differentiate attogram level stroked antigen and the vehicle alcohol patterns (Figure 8), probably due to low sensitiveness.

Statistical Analysis

Besides gene expression patterns by graphical representations, we also studied the correlations and

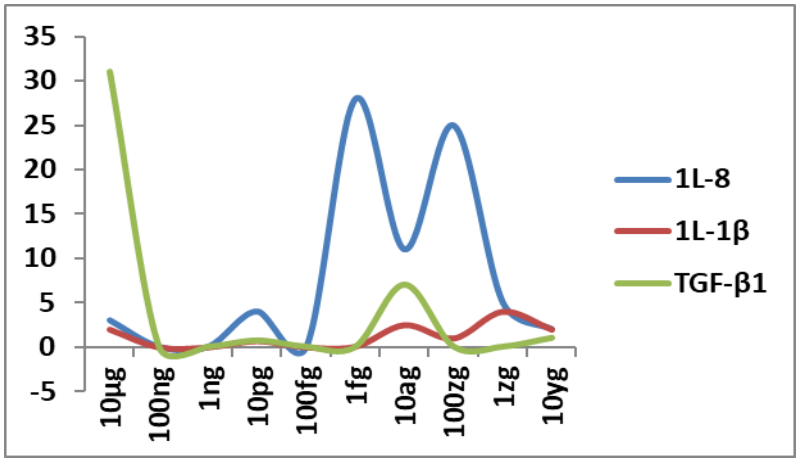

Figure 4. IL-8, IL-1β, and TGF-β1 gene expression changes (Y-axis) at 48h with different concentrations of Delta spike protein RBD antigen of SARS-CoV-2 in allantoic fluid of embryonated egg; fg-femtogram, ag-attogram, zg-zeptogram, yg-yoctogram.

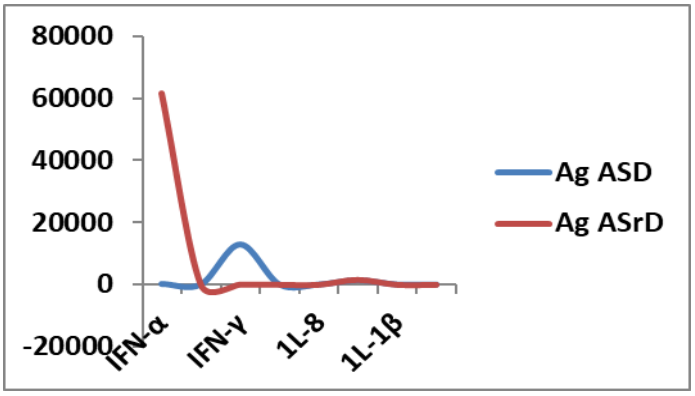

Figure 5. Cytokine gene expressions (Y-axis) with stroked antigen (Ag ASrD) and non-stroked antigen (Ag ASD) at attogram level at 48h in allantoic fluid of embryonated eggs. IFN-α gene expression was markedly increased with Ag ASrD, while IFN-γ gene expression was significantly increased with AgASD. Other cytokine gene expressions were comparable.

Table 1. Gene expression levels (fold increase considering normal control values as 1) of different cytokines in amniotic fluid studied in this experiment in different experimental sets.

	Alcohol	Attogram level stroked antigen	Pre-experimental set	Post experimental set	Original Antigen
INF-α	0.54	3.05	0.21	0.61	0.94
INF-β	0.57	2.60	0.20	0.68	0.68
INF-γ	2.33	3.75	1.09	0.74	0.00
IL-6	0.00	59.52	66.95	297.49	369.78
IL-8	0.02	1.54	2.42	5.60	16.93
IL-10	0.00	0.16	0.26	0.18	0.85
IL-1β	0.02	0.16	2.85	4.76	10.39
TGF-β1	0.45	0.53	0.71	0.34	0.15

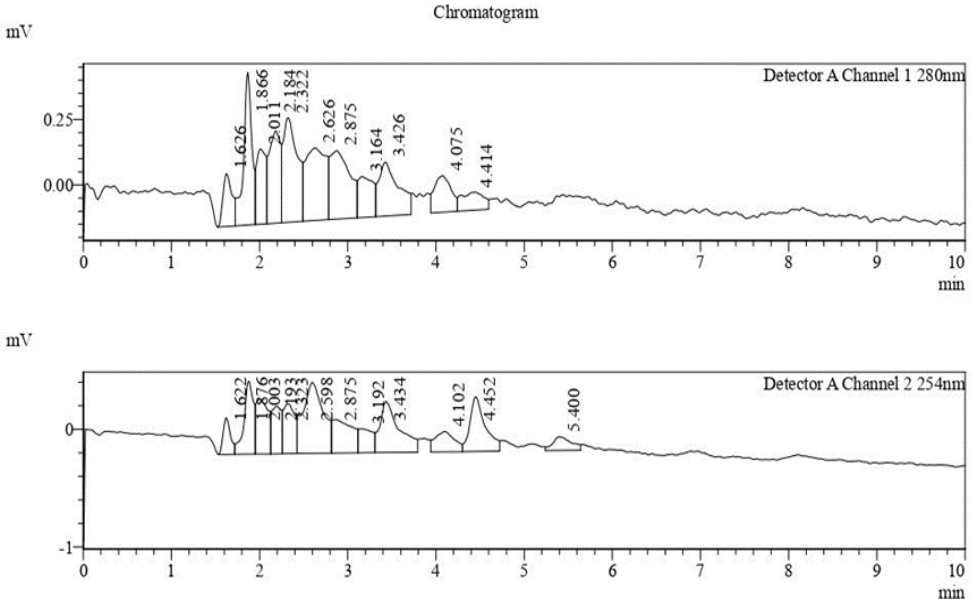

Peak Table

Detector A Channel 1 280nm

Peak#	Ret. Time	Name	Area	Height
1	1.626		1445	201
2	1.866		3844	581
3	2.011		2124	287
4	2.184		3134	353
5	2.322		4471	399
6	2.626		4463	277
7	2.875		4083	261
8	3.164		1795	157
9	3.426		3195	206
10	4.075		1850	139
11	4.414		1233	69
Total			31637	2930

Figure 6. HPLC study of ultra diluted (attogram level) stroked antigen in alcohol. The chromatogram showed trace amount of chemicals with 11 peaks.

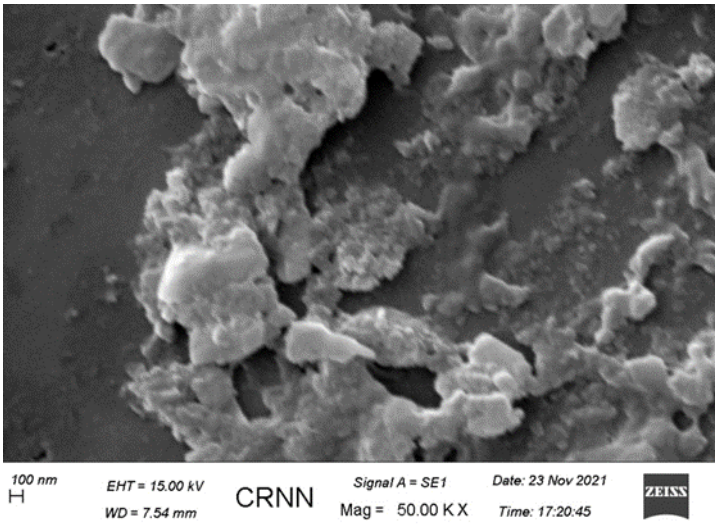

Figure 7. SEM study of attogram level stroked antigen in alcohol. It indicates the presence of many nanoparticles originating from the antigen molecules along with some larger particles of silica probably originated from the surface of the glass container during strokes.

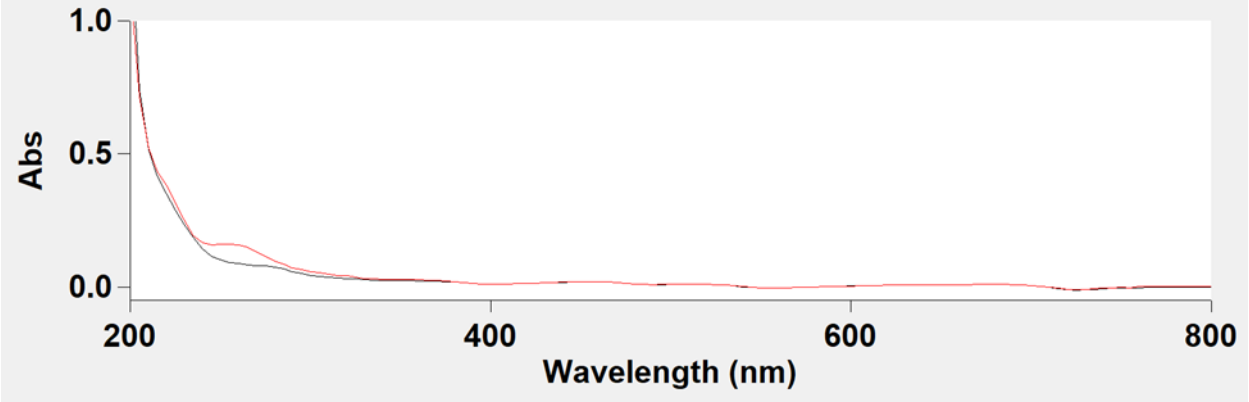

Figure 8. UV-Spectroscopy pattern of attogram level stroked antigen in alcohol (blue colour). There is practically no difference with the vehicle ethanol (red colour).

regression equations of different cytokine expressions between experimental sets. For analysis, the eight cytokines were numbered I to VIII (I: INF-α, II: INF-β, III: INF-γ, IV: IL-6, V: IL-8, VI: IL-10, VII: IL-1β, VIII: TGF-β1). In the first step, a pair-wise Pearson Correlation matrix was prepared. The analysis indicated a very high correlation between gene expressions of IL-6 and IL-8 (p-value 0.002); IL-10 and IL-1β (p-value 0.001); INF-α and INF-β (p-value 0.005) in between different experimental sets (Supplementary file: Statistical analysis).

Discussion

One may expect mouse as an animal model for pre-clinical study in COVID-19. Two important mouse models are used to study SARS-CoV-2 pathogenic changes: the human ACE-2 transgenic mouse model and the adenovirus-assisted human ACE-2 transduction mouse model. However, pathogenic changes are mild in these models, without indicating signs of the disease and good virus replication. A biosafety level-3 is also required for such experimental studies [15,16]. Thus we have yet to find a mouse model which can quickly delineate Covid-19 pathogenic changes.

Artificial incubation of chicken eggs was first practised by Egyptians as early as 1400 BC, and Aristotle did the first experimental study on chick embryos in 350 BC. William Harvey studied the blood vessels of the chick embryo in 1628. In 1906, Constantin Levaditi first used the chick embryo model to study infections. Francis Peyton Rous shared Nobel Prize in 1966 for his 1911 study of Rous Sarcoma Virus (RSV) in the chick embryo, and the most important observation of routine cultivation of viruses in chick embryo was made in 1931 by Ernest William Goodpasture and Alice Miles Woodruff when they published their protocol of fowl-pox virus cultivation. The famous virologist Sir Frank Macfarlane Burnet declared, "Nearly all the later practical advances in the control of virus diseases in man and animals sprang from this single discovery". Thus we have seen vaccinia, pox, herpes simplex, Usutu, influenza, paramyxo, yellow fever, rabies, Newcastle disease, mumps, and many mammalian and avian viruses are cultivated successfully and used for the production of vaccines in this model.

Other scientists used the chick embryo model to study bacteria, fungi, parasites, growth and spread of cancers, genomic changes, blastoderm culture, nerve growth factors, contact inhibition, and developmental and immunological changes [17]. Naturally ideal substrates for growth and replication of viruses, relatively immature immune system, good vasculature and angiogenesis, sterile environment, limited legal and ethical issues (no ethical issue up to 18 days), easy availability, and simple experimental interventions lead to the recognition it at present as an experimental model of choice, by many scientists throughout the globe. Recently the nasal spray vaccine against COVID-19 developed at Icahn School of Medicine at Mount Sinai in New York City (formerly the Mount Sinai School of Medicine) has been developed in eggs.

It is challenging to state the exact mechanism of such cytokine changes in embryonated eggs. If we observe published papers, it has been demonstrated that when challenged with SARS-CoV-2, chickens are not infected, and there is no sign of infection in them. In an experiment by Barr et al. [18] in embryonated eggs, it was found that the number of viruses was markedly decreased in the first passage in both amniotic and allantoic routes. It probably indicates that the chicken ACE2 receptor differs from human ACE2 receptors—three of the five critical residues of ACE2, viz. Lys31Glu, Glu35Arg, and Met82Arg are altered in chicks [19]. However, inefficient egg replication indicates multiple restrictions in different steps instead of one binding site, which is not adequately explored. The per cent sequence identity of chick ACE2 across all amino acids of human ACE2 (full-length ACE2) is 66.25%, and with interacting residues, this is only 52% [20]. Phylogenetic analysis of chicken based on ACE2, and characteristics of the SARS-CoV-2 twenty different crucial residues of human ACE2 binding with SARS-CoV-2 RBD, indicated 50% similarity and 50% substitution [21]. Thus all these points suggest that some prominent priming of SARS-CoV-2 RBD protein for binding occurs by some proteases in the absence of S-2 fusion protein, which enable these remarkable changes. Thus unless RBD protein and Chick ACE2 binding are adequately explored, it is difficult to explain in the present scenario.

It is the cytokine network responsible for cross-talk between cells in a biological system for their development and regulation. Each cytokine produces effects on different target cells after modulation by other cytokines. This is possible due to multimeric cytokine receptors and transduced signal determination after ligand binding. Based on the structures of their receptors, cytokines are broadly classified into four different types. Type I cytokine receptor family, or hematopoietin receptor family, includes IL-2 to IL-7, IL-9, IL-11, IL-12, IL-15, GM-CSF, G-CSF, LIF, OSM, CNTF, CT-1, thrombopoietin, growth hormone, prolactin, and erythropoietin. There are high-affinity receptors composed of α and β chains. The Alpha chain is the cytokine-specific subunit. The three types of α chain compete for the β chain to form a high-affinity receptor. In all other complex receptor systems, this phenomenon is active, e.g. gp130, a common receptor for IL-6, LIF, OSM, CNTF, IL-11, and CT-1. Type II cytokine receptor family includes IFN α, IFN β, IFN γ, and IL-10. They have a similar pattern in their 210 amino acid extracellular domain. Type III cytokine receptor family or TNF receptor family belongs to two groups- death receptors (DRs): Fas/Apo-1, TNFR-1, DR-3, TRAIL receptors, and other receptors: TNFR2, NGF, etc. Type IV cytokine receptor family includes IL-1 and its related receptors. There are some other receptor groups, e.g. chemokine receptor groups etc.

Dimerization or oligomerization occurs during the binding of cytokines to their specific receptors. Following this, Jak kinases usually phosphorylate each other, opening numerous docking sites for proteins with the activation of multiple signal transduction pathways. Jak1, Jak2, Jak3, and Tyk2 are activated by different cytokines, usually with a combination of Jaks. IL-6 uses Jak1, Jak2 and Tyk2; IFN-γ uses Jak1 and Jak2 etc. STATs latent cytoplasmic transcription factors after phosphorylation translocate to the nucleus and interact DNA-binding site. STATS are much less in number than cytokine receptors. In general, cytokines control cell survival, proliferation, differentiation, and cell death.

It is well known that the naïve T cells can produce only IL-2, but when it differentiates in Th1 and Th2 cells, Th1 cells induce cellular immunity while Th2 cells secrete IL-4, IL-5, IL-6, and IL-10. They help in antibody formation by B cells. However, it is IL-2 that mainly acts in immunoglobulin synthesis. IL-4 and IL-10 help in immunoglobulin synthesis in the absence of IL-2.

IL-6 is produced by B cells, T cells, monocytes, endothelial cells, and fibroblasts. IL-6 gene is present in chromosome 7p21 with five exons and four introns. IL-6 cDNA is 1.1 kb long with ORF 636 bp. IL-6 is secreted by macrophages in response to specific microbial molecules, referred to as pathogen-associated molecular patterns (PAMPs). These PAMPs bind to an essential group of detection molecules of the innate immune system, called pattern recognition receptors (PRRs), including Toll-like receptors (TLRs).

Now, if we look at the IL-10 changes, it appears very significant. Glucocorticoids, cyclosporine A, chlorpromazine, phosphodiesterase type IV inhibitors like Rolipram, compounds that increase intracellular cAMP (epinephrine, PGE2, pentoxifylline), NF-Kb activators (HIV-1, EBV, ROS, UV light, TNF-α) up-regulate IL-10 levels. Tellurium-based antitumor compounds like AS101 can down-regulate IL-10 synthesis. IL-10 diminishes formation of pro-inflammatory cytokines IL-1α, IL-1-β, IL-6, IL-8, TNF-α, G-CSF, GM-CSF and chemokines. When activated human monocytes produce large amounts of IL-10, it inhibits APC function by down-regulating MHC class II. It promotes the B lymphocytes' synthesis of IgM, IgG, and IgA. IL-10 can also control inflammatory processes of allergic origin.

In this study, interferon changes were also found very prominent. Isaacs and Lindenmann first used the term interferon in 1957 to describe the protection of cells from subsequent viral infection by supernatant of viral infected cell culture. A viral infection of cells induces type I interferons. Leukocytes and macrophages produce 21 varieties called interferon α or IFN-α. In contrast, a single kind of Type I interferons is produced by fibroblasts and epithelial cells and is known as IFN-β. The Type II interferon is IFN-γ which is not produced by a viral infection but generated as a result of stimulation of T lymphocytes and NK cells. IFN-γ gives a wide range of protection, including its antiviral activities in comparison to Type I interferons and is an excellent immunomodulatory agent.

Type I interferon induction is a rapid phenomenon, and IFN-α/IFN-β can be detected within 6h after cellular stimulation. IFN-γ level reaches the maximum at 18-24h after T-cell stimulation. IL-10 is an indirect negative regulator of IFNγ from T and NK cells. Interferons are involved in antiviral, antiproliferative, macrophage activation, antigen processing, presentation, development of T-helper cell phenotype, regulation of humoral immunity, and tumour immunity.

In this study, changes in IL-1β and TGF-β1 were not prominent: There are three isomers of TGF: TGF-β1, THF-β2 and TGF-β. Although most cells can produce TGF-β, platelets, bone, and spleen are the essential sources of TGF-β. The main activities are chemotaxis stimulation, extracellular matrix formation, cell growth, and differentiation.

In previous experiments, it was proved that high dilutions of aspirin showed aggregate and prothrombotic activities [22]. When neuronal cells are exposed to ultra-diluted glutamate, they are protected from a toxic dose of glutamate [23]. High dilution of As2O3 increases the elimination of arsenious anhydride [24], and High dilutions of histamine prevent basophil degranulation [25].

It is important to note that the biological action of ultra-diluted solutions is highly controversial. Although we shall give some explanations of our findings, we are also not in a position to explain our interesting findings firmly. Still, it is essential to note that the results were identical in all our repeat experiments.

In this paper, we observed ultra-diluted alcosols showing unexpected changes in cytokines. There are many interesting views on how ultra-diluted chemicals impart biological activities. In this connection, we may recall Einstein's paper on the Brownian movement (1905), in which he mentioned that "colloid acts like atom", indicating structuring of the vehicle [26] by the charged solid phase. Thus with the development of a di-phasic alcosol, the stable protein molecules will act as templates for such structuring leading to enhanced receptor bindings, molecular cascade phenomenon, and enhanced genetic modulation of bioactive cytokines.

In a protein solution, when concentration is more, molecular crowding, phase separation, aggregation, and viscosity influence the protein interactions [27]. The second osmotic virial coefficient (B22) indicates a measurement of non-ideal solution behaviour in two-phase interactions. It is significant in ultra-diluted protein solutions depending on electrolytes and pH. The reverse Kirkwood-Buff solution theory is also crucial to explain these exceptional results.

SARS-CoV-2 mainly affects the respiratory system; however other organs may also get involved, and this causes

multi-organ failure. The infection in the lower respiratory tract causes symptoms such as fever, dry cough, and dyspnea, along with headache, dizziness, generalized weakness, vomiting, and diarrhoea. Severely infected patients demonstrated enhanced concentrations of proinflammatory cytokines within the plasma, including IL-6, IL-10, G-CSF, MCP1, MIP1 α, and TNF-α. In some patients, disease progression leads to an enormous secretion of cytokines, known as cytokine storm; among those cytokines, IL-6 plays an important role. The primary activators of the IL-6 expression are IL - 1β and TNFα; many other factors can contribute to its secretion, such as Toll-like receptors (TLRs), prostaglandins, adipokines, stress response, etc. In the early stage of infectious inflammation, IL-6 is produced by monocytes and macrophages stimulated by the TLRs.

Although different pharmaceutical industries are giving updates on their COVID-19 vaccines tailored to protect against new viral variants, in the long run, it would be challenging due to time constrain and expense. Thus, if we follow this simple technique in a generalized way in different viral infections, it may help in treating such diseases. However, we have to go a long way toward an important conclusion like this.

Conclusion

It is well known that the Delta strain of SARS-CoV-2 is highly infectious compared to other mutated strains of this virus. It is also well known that mutations of the RBD region of the spike protein are most important regarding the generation of new strains. Some evidence is there that dangerous chemicals behave differently in extremely diluted conditions. Thus in this experiment, we observed whether the ultra diluted Delta SARS-CoV-2 RBD spike protein could act differently than the spike protein in relatively higher concentrations. In this experiment, diluted antigens up to yoctogram levels were administered in 14 days old *Gallus gallus* embryonated eggs through the amniotic route. We selected *Gallus gallus* embryonated eggs because they are not only enriched with ACE2 receptors (~75% similarity with hACE2), but they also contain a very high amount of NRP1 receptors for binding with RBD S protein. After the initial experiment, we selected the most effective attogram level diluted antigen for the final study. INF-α gene expression was remarkably increased at the attogram, and zeptogram level diluted antigens. IL-10 gene expression was more than IL-6 gene expression at attogram antigen levels. Pre-experimental set, where attogram level antigen was introduced first followed by microgram level antigen, showed better results concerning cytokine balance. This observation proves that ultra diluted Delta SARS-CoV-2 RBD spike protein at attogram level may maintain cytokine balance under challenging situations and opens our future vision of whether similar changes may occur in other viral diseases when specific antigens are used in highly diluted forms.

Acknowledgement

We acknowledge Mr Pradip Agarwal, Chief Executive Officer, Heritage Institute of Technology, Kolkata, India, and Dr Sajjan Bhajanka, Member, Kalyan Bharti Trust, for providing infrastructure and facilities for this study.

Author Contribution

SD (Conceptualization, methodology, supervision, validation, writing original draft, editing, approval), DC (Investigation, data collection, formal analysis), KP (Project administration, resources, investigation)

Ethical Issue

The study was approved by HIT Institutional Ethical Committee, Kolkata.

Funding

The Authors declare that no funds, grants, or other support were received during the preparation of this manuscript.

Conflict of Interests

The Authors have no relevant financial or non-financial interests to disclose.

Data Availability Statement

All data included in the manuscript will be available.

Informed Consent

Not applicable in this study.

Abbreviations

ACE2 (angiotensin-converting enzyme 2), APC (Antigen presenting cell), APN (aminopeptitase N), cAMP (Cyclic adenosine monophosphate), CEACAM (carcinoembryonic antigen -related cell adhesion molecule-1), CNTF(Ciliary neurotrophic factor), CT-1(Cardiotrophin-1), dNTP (deoxy nucleoside triphosphate), DPP4 (dipeptidyl peptidase-4), EBV (Epstein Barr Virus), G-CSF(Granulocyte colony stimulating factor), GM-CSF(Granulocyte-macrophage colony stimulating factor), INF-α (Interferon alpha), INF-β (Interferon Beta), INF -γ (Interferon Gamma), IL-6 (Interleukin 6), IL-8 (Interleukin 8), IL-10 (Interleukin 10), IL-1β (Interleukin 1 Beta), IP-10 (Interferon gamma induced protein-10), Jak (Janus kinase), LIF(Leukemia inhibitory factor), MIP (Macrophage inflammatory protein), MCP (Monocyte chemoattractant protein), NGF (Nerve growth factor), O-acSia (O-acetylated sialic acid), OSM (Oncostatin M), PBS (Phosphate buffered saline), ROS (Reactive oxygen species), Sia (sialic acid), SDS-PAGE (Sodium dodecyl sulfate polyacrylamide gel electrophoresis), SEM (Scanning electron microscope), STAT (Signal transducer and activator of transcription), TGF-β1 (Transforming growth factor beta 1), TNF (Tumor necrosis factor), TNFR (Tumor necrosis factor receptor) TRAIL (Tumor necrosis factor related apoptosis inducing ligand), Tyk2 (Tyrosine kinase 2).

References

1. Brauner JM, Mindermann S, Sharma M, Johnston D, Salvatier J, Gavenčiak T, Stephenson AB, Leech G, Altman G, Mikulik V, Norman AJ, Monrad JT, Besiroglu T, Ge H, Hartwick MA, Teh YW, Chindelevitch L, Gal Y, Kulveit J. (2021), Inferring the effectiveness of government interventions against COVID-19, Science, 371(6531),doi: 10.1126/science.abd9338.
2. Allen K, Buklijas T, Chen A et al, (2020), Tracking global evidence-to-policy pathways in the coronavirus crisis: a preliminary report. Auckland.
3. Skegg D, Gluckman P, Boulton G, Hackmann H, Karim SSA, Piot P, Woopen C. (2021), Future scenarios for the COVID-19 pandemic. Lancet. 397(10276):777-778. doi: 10.1016/S0140-6736(21)00424-4.
4. Bhargava P, Panda P, Ostwal V, Ramaswamy A. (2020), Repurposing valproate to prevent acute respiratory distress syndrome/acute lung injury in COVID-19: A review of immunomodulatory action. Cancer Res Statistics Treat, 3 (5):65. doi: 10.4103/ CRST.CRST_156_20
5. Oberfeld B, Achanta A, Carpenter K, Chen P, Gilette NM, Langat P, et al. (2020), SnapShot: COVID-19. Cell, 181 (4):954–e1. doi: 10.1016/j.cell. 2020.04.013
6. Qin C, Zhou L, Hu Z, Zhang S, Yang S, Tao Y, et al. (2020), Dysregulation of immune response in patients with COVID-19 in Wuhan, China. Clin Infect Dis: An Off Publ Infect Dis Soc America,71(15):762–8. doi: 10.1093/cid/ ciaa248
7. Tan M, Liu Y, Zhou R, Deng X, Li F, Liang K, et al. (2020), Immunopathological characteristics of coronavirus disease 2019 cases in Guangzhou, China. Immunology, 160(3):261–8. doi: 10.1111/imm.13223
8. Tai, W., He, L., Zhang, X. et al. (2020), Characterization of the receptor-binding domain (RBD) of 2019 novel coronavirus: implication for development of RBD protein as a viral attachment inhibitor and vaccine. Cell Mol Immunol, 17, 613–620. https://doi.org/10.1038/s41423-020-0400-4
9. Jiang S, Hillyer C, Du L, (2020), Neutralizing Antibodies against SARS-CoV-2 and Other Human Coronaviruses, Trends in Immunology, 41: 5, 355-359, ISSN 1471-4906, https://doi.org/10.1016/j.it.2020.03.007.
10. Walls A C, Park Y-J, Tortorici M A, et al., (2020), Structure, Function, and Antigenicity of the SARSCoV-2 Spike Glycoprotein, Cell, 180, 281–292. https:// doi.org/10.1016/j.cell.2020.02.058
11. Walls, A.C., Tortorici, M.A., Bosch, B.J. et al. (2016), Cryo-electron microscopy structure of a coronavirus spike

glycoprotein trimer. Nature, 531(7592), 114-117.

12. Yang, J., Wang, W., Chen, Z. et al. (2020), A vaccine targeting the RBD of the S protein of SARS-CoV-2 induces protective immunity. Nature, 586, 572–577. https://doi.org/10.1038/s41586-020-2599-8
13. van Loggerenberg F, Mlisana K, Williamson C, Auld SC, Morris L, Gray CM, Abdool Karim Q, Grobler A, Barnabas N, Iriogbe I, Abdool Karim SS; (2008), CAPRISA 002 Acute Infection Study Team. Establishing a cohort at high risk of HIV infection in South Africa: challenges and experiences of the CAPRISA 002 acute infection study. PLoS One., 3(4):e1954. doi: 10.1371/journal.pone.0001954.
14. Arnold KB, Burgener A, Birse K, Romas L, Dunphy LJ, Shahabi K, Abou M, Westmacott GR, McCorrister S, Kwatampora J, Nyanga B, Kimani J, Masson L, Liebenberg LJ, Abdool Karim SS, Passmore JA, Lauffenburger DA, Kaul R, McKinnon LR. (2016), Increased levels of inflammatory cytokines in the female reproductive tract are associated with altered expression of proteases, mucosal barrier proteins, and an influx of HIV-susceptible target cells. Mucosal Immunol. 9(1):194-205. doi: 10.1038/mi.2015.51.
15. Neerukonda SN, Katneni U. (2020), A Review on SARS-CoV-2 Virology, Pathophysiology, Animal Models, and Anti-Viral Interventions. Pathogens, 9(6):426. doi: 10.3390/pathogens9060426
16. Sun SH, Chen Q, Gu HJ, Yang G, Wang YX, Huang XY, et al. (2020), A Mouse Model of SARS-CoV-2 Infection and Pathogenesis. Cell Host Microbe, 28 (1): 124–33.e4. doi: 10.1016/j.chom.2020.05.020.
17. Leupold J.H., Patil N., Allgayer H. (2021), The Chicken Egg Chorioallantoic Membrane (CAM) Model as an In Vivo Method for the Investigation of the Invasion and Metastasis Cascade of Malignant Tumor Cells. In: Stein U.S. (eds) Metastasis. Methods in Molecular Biology, vol 2294. Humana, New York, NY. https://doi.org/10.1007/978-1-0716-1350-4_2
18. Barr IG, Rynehart C, Whitney P, Druce J. (2020), SARS-CoV-2 does not replicate in embryonated hen's eggs or in MDCK cell lines. Euro Surveill. 25(25):2001122. doi:10.2807/1560-7917.ES.2020.25.25.2001122
19. Swayne DE, Suarez DL, Spackman E, et al. (2004), Domestic poultry and SARS coronavirus, southern China. Emerg Infect Dis. 10(5):914-916. doi:10.3201/eid1005.030827
20. Low-Gan J, Huang R, Kelley A, Jenkins G W, McGregor D, Smider V V; (2021), Diversity of ACE2 and its interaction with SARS-CoV-2 receptor binding domain. Biochem J , 478 (19): 3671–3684. doi: https://doi.org/10.1042/BCJ20200908
21. Wu L, Chen Q, Liu K, et al. (2020), Broad host range of SARS-CoV-2 and the molecular basis for SARS-CoV-2 binding to cat ACE2. Cell Discov. 6:68. doi:10.1038/s41421-020-00210-9.
22. Doutremepuich C, Aguejouf O, Pintigny D, Sertillanges MN, De Seze O. (1994), Thrombogenic properties of ultra low dose of acetylsalicylic acid in a vessel model of laser induced thrombus formation. Thrombosis Research, 76; 2: 225–9.
23. Jonas WB, Lin Y, Tortella F. (2001), Neuroprotection from glutamate toxicity with ultra-low dose glutamate. Neuroreport, 12: 335–9.
24. Cazin JC, Cazin M, Gaborit JL, Chaoui A, Boiron J, Belon P et al. (1987), A study of the effect of decimal and centesimal dilutions of arsenic on the retention and mobilization of arsenic in the rat. Human Toxicology, 6: 315–20.
25. Sainte-Laudy J, Belon P. (1993), Inhibition of human basophil activation by high dilutions of histamine. Agents Actions, 38: C245–7.
26. Rao ML, Roy R, Bell I. (2008), Characterization of the structure of ultra dilute sols with remarkable biological properties. Mater Lett. 62(10-11):1487. doi:10.1016/j.matlet.2007.09.007
27. Saluja, A.; Kalonia, D. S. (2008), Nature and Consequenc-

es of Protein– Protein Interactions in High Protein Concentration Solutions. Int. J. Pharm. 358, 1–15.